2020 3rd IEEE International Conference on Soft Robotics (RoboSoft)
Yale University, USA

Scalable Tactile Sensing for an Omni-adaptive Soft Robot Finger*

Zeyi Yang[1,#], Sheng Ge[1,#], Fang Wan[2], Yujia Liu[1], and Chaoyang Song[3,*]

***Abstract*— Robotic fingers made of soft material and compliant structures usually lead to superior adaptation when interacting with the unstructured physical environment. In this paper, we present an embedded sensing solution using optical fibers for an omni-adaptive soft robotic finger with exceptional adaptation in all directions. In particular, we managed to insert a pair of optical fibers inside the finger's structural cavity without interfering with its adaptive performance. The resultant integration is scalable as a versatile, low-cost, and moisture-proof solution for physically safe human-robot interaction. In addition, we experimented with our finger design for an object sorting task and identified sectional diameters of 94% objects within the ±6mm error and measured 80% of the structural strains within ±0.1mm/mm error. The proposed sensor design opens many doors in future applications of soft robotics for scalable and adaptive physical interactions in the unstructured environment.**

***Index Terms*— soft robot, tactile sensing, optical fiber, adaptive grasping**

I. Introduction

Robotic devices made of soft components not only exhibit superior adaptation in actuation [1], but also in sensing [2]. Previous research on tactile sensing usually requires an explicit understanding of the material mechanics to build analytical models that translate structural deformation into sensory data [3], [4]. However, the non-linear mechanics inherently involved in the soft material remains a challenging issue in the kinematic analysis and dynamic modeling of soft robot [4]–[7]. On the other hand, recent research has shown novel tactile sensing solutions using soft robots through the integration with other devices, such as visual sensors [8].

However, modeling the deformation of a soft structure is challenging. Numerous analyses and calculations were implemented to simulate a simple soft structure [5]. The traditional sensing technology to evaluate the strain is using a strain gauge, which takes advantage of the properties of electrical principle [9], which requires the integration of the gauge in the fingers. Piezoresistance is a scalable and low-cost sensory element to generate tactile perception, but it also needs electrical arrays to support and is challenging to measure the bending state directly [10], [11]. Also, waterproofing must be considered, in case we use the gripper in a wet environment or even underwater, which is more challenging during tactile sensing integration.

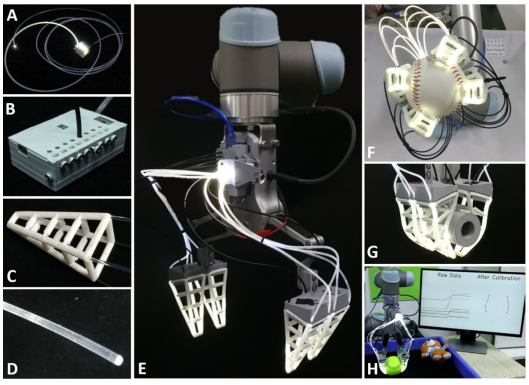

Fig. 1: Overview of scalable sensing design of gripper and sensors. The sensor system includes a strong LED light source (A), a microprocessor box (B), soft fingers (C), and optical fiber (D), which is installed on a real robot arm UR5 (E). Each finger will passively adapt to a baseball (F) while grasping, especially be effective for cylindrical objects (G). The final integration of sensor with gripper can achieve detecting the horizontal section in real time (H).

A. Related Work

Recent research about the tactile sensor for soft robots focuses on innovations relating to scalability and engineering potentials [12]. The tendency of using neural networks to process high-dimensional sensory data is widely accepted by researchers, which provide a more accurate model via repetitious training [3], [8], [13], [14]. However, the traditional calibration method is also applied by some sensors and shows good results [10], [11]. Piezoresistive is an appropriate component for tactile sensing on soft robot [15], its application on a perceptive glove shows the scalability on tactile sorting [13]. A handmade capacitive stack-up sensor was tested and applied on an object sorting experiment [10], which is directly attached to a finger of handed shearing auxetic cylinders [16].

Optical sensing has been widely researched for its ease of integration with soft robots. An innovative method to detect the deformation of soft prosthetic hand via stretchable optical waveguides shows the prospect of an optical sensor [11]. A plastic optical fiber pressure sensor [17] was presented as the merits of low cost and simple fabrication. Moreover, recent

*This work was supported by Southern University of Science and Technology and AncoraSpring Inc.

[1]Zeyi Yang, Sheng Ge, and Yujia Liu are with Department of Mechanical and Energy Engineering, Southern University of Science and Technology, Shenzhen, Guangdong 518055, China. 11610518, 11612122, liuyj@mail.sustech.edu.cn

[2]Fang Wan is with AncoraSpring, Inc. and currently a visiting scholar at SUSTech Institute of Robotics, Southern University of Science and Technology, Shenzhen, Guangdong 518055, China. sophie.fwan@gmail.cn

[3]Chaoyang Song is the corresponding author with the Department of Mechanical and Energy Engineering, Southern University of Science and Technology, Shenzhen, Guangdong 518055, China. songcy@ieee.org

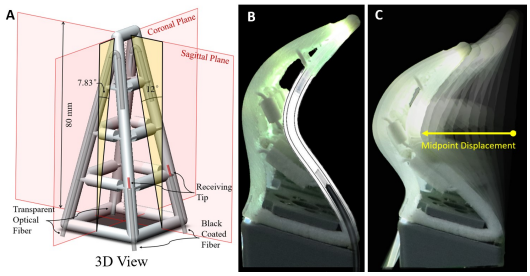

Fig. 2: Soft finger and sensor design. The Sagittal plane and Coronal plane are the main bending planes (A). The soft optical fiber passes through the inner tube to transmit the light which will be received by a black coated optical fiber (A). The tube wall will hinder light transmission while bending (B), which relate to the midpoint displacement (C).

research about applying soft optoelectronic sensory foams presented an extremely accurate estimated 3D-model for the entire deformation of a regular soft foam [14]. Most recent research using optical lace also opens a window for soft robot tactile sensing [8] using the contact of input fiber and distributed output fibers, which are inserted in a 3D-printed elastomer.

The soft grippers as the base of the tactile sensor have a variety of designs with diverse functions [18]. An embedded tactile sensor enables more functions for the gripper, such as closed-loop object picking [19]. Besides, the sorting experiment is a good verification for the properties of soft robotic fingers with tactile sensing. The application of fingers with the structure of handed shearing auxetic showed excellent examples of object sorting and material classification [10], [20].

B. Proposed Method and Contributions

In this paper, we propose a scalable, embedded tactile sensing solution using soft optical fiber inside a novel design of soft robot finger with passive, omni-directional adaptation, as shown in Fig. 1. While most tactile sensing solutions are usually considered as a subsystem independent of the overall robot, our proposed design is seamlessly integrated inside this unique network structure of the soft robotic finger without impeding its omni-adaptive performance. We managed to capture the three-dimensional geometric deformation through a scalable sensing solution using soft optical fiber. The major contributions of this paper are listed as the following.

- An integrated design of the fiber-cavity sensor with an omni-adaptive soft finger.
- Extensive experiment and characterization of the fiber-cavity senor.
- Sensor implementation in sorting tasks of daily objects via an integrated gripper system.

II. Embedded Tactile Sensing for Scalability

A. Soft Finger Network for Omni-adaptation

In this paper, we adopt a novel design of soft finger networks with passive adaptation in all directions of physical contact. Fig. 2A shows the three-dimensional (3D) view of the soft finger network, where layers of squared shapes with the shrinking area are stacked on top of the other with links on the sides to connect them, forming the basic structure of this finger design. When fabricated with soft material, such as silicone rubber or Thermoplastic Urethane (TPU), the 3D structure is capable of passive adaptation of the overall structural geometry, as shown in Figs. 2B & C. Due to the hollowed squares used, the finger achieves omni-directional adaptation instead of a uni-directional response. One can design any shape for each of the layers as long as a specific hollow can be kept near the certain of each layer for geometric adaptation.

B. Embedded Optical Fiber for Scalable Tactile Sensing

Given the omni-adaptive nature of this soft finger network, we set our sensor design with a goal of minimum interference with its geometric adaptation without limiting its usage scenario. As a result, the optical fibers are selected for several reasons. First, the material property of the optical fibers is very similar to that of some materials used for this soft finger network. Second, optical sensing is capable of robust measurement over a long distance, and the optical sensor is not placed in the finger structure, but outside of it near the gripper base. As a result, we can still apply such soft finger design in the same operational environment without worrying about the protection of the sensing electronics on the finger. Finally, optical fibers are a relatively cheap solution when scalability is taken into considerations.

We implement the resultant sensor design by creating a cavity with the structural supporting beams between each finger layer and then embedding the optical fibers inside to capture the geometric deformation. The transmitting fiber is different from the receiving fiber. The core of transmitting optical fiber (Model hof-2, EverHeng Optical Co., Shenzhen, China) is 2mm polymethyl methacrylate (PMMA) fiber, which has a 0.2-0.5db/m attenuation rate, and with a cladding of transparent polytetrafluoroethylene (PTFE) outside. The receiving fiber (Model epef-1.5) is 1.5mm PMMA core with PTFE cladding and additional black polyvinyl chloride (PVC) jacket. For example, in the soft finger structure with four supporting beams shown in Fig. 2, the cylindrical cavity is designed inside each of the beams matching the diameter of the optical fiber. From the side-viewing angle in Fig. 2B, the transmitting optical fiber with a light source is inserted from the base of one beam at the backside of interaction. Then, the receiving optical fiber is inserted through another beam at the front side of interaction to its base, where photo-resistance sensors (Model GL5506) are installed. During bending motions, the reading from the sensors corresponds to the number of geometric deformations inside the front side beams of interaction. When the backbones bend in a direction, the received light intensity will attenuate theoretically because of being hindered by the deformation of the tube wall. We named the sensor as a fiber-cavity sensor. Also, the length of the inner cavity needs to be carefully selected. After several testing, 35mm shows a satisfying result of

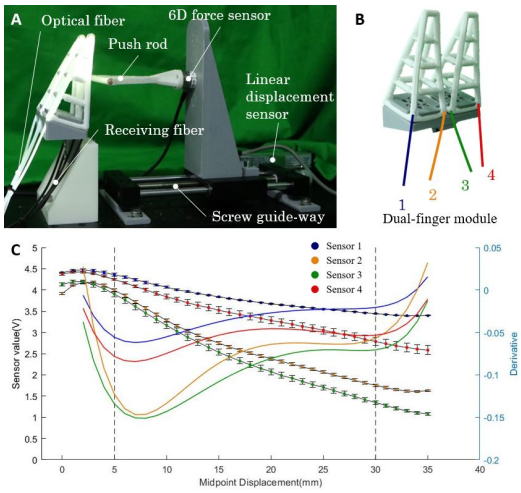

Fig. 3: Experimental platform (A) and data from fiber-cavity sensors. The half of gripper is a dual-finger model with four-channel of fiber-cavity sensor (B), which was directly used in the experiment. The graph is about the raw data of sensors (line with square and error bar) and its derivative (thinner fine line) after filtering (C).

performance. Too long or too short will cause a reduction of the measurement range.

III. Sensor Characterization

Given the nature of our integrated sensor design, the experiment setup is closely related to observations of the soft finger network under loading. Besides the pure bending behavior at the normal surface, the omni-directional adaptation relies greatly on the twisting deformation at random angles to the finger surface, which is essentially a differential reading from the two contacting beams. As a result, we set up our experiment characterization by measuring the force normal to the finger surface, as shown in Fig. 3A. A T-shape rod is fixed on top of a manual linear guide-way to push the midpoint of the finger at a right angle as the displacement input. A 6D force and torque sensor (ATI Nano 17) is fixed at the end of the T-shape rod for measuring the output force. Optical sensor readings are also recorded for sensor characterization and calibration.

In this experiment, two such soft finger networks are mounted at the same time, which is the same as the ones to be installed on one of the fingertips of the robotic gripper to be used later. A total of four sets of fiber-cavity sensor readings are recorded in Fig. 3B with results reported in Fig. 3C. We definite the original point of displacement at the midpoint of the backbone in the non-grasping state. The positive direction is towards the back surface. The sensor value is a voltage from 0v to 5v, which positively correlates with the light intensity. Each measurement is repeated three times, and the standard error bars are also included.

We identify three stages of behaviors from the results in Fig. 3C between a measurement range of 0-35mm displacement range. For the initial stage up to around 5mm displacement at finger midpoint, the small bending behaviors of the soft finger network is not well-captured by the fiber-cavity sensors. The diffuse reflection of the light by the tube wall causes the photo-transduction instability, invalidating sensor readings at this stage. For the final stage beyond 30mm displacement at finger midpoint, although the soft finger network still shows adaptive behaviors, the inner layers start to stack on top of each other, as shown in Fig. 2C, making it challenging to produce consistent sensor readings. Sensors readings during this stage are also disregarded by one can still utilize the twisting behavior at this stage for grasping an object of irregular shape.

During the stable stage between 5-30mm displacement at finger midpoint, the recorded results show good linearity between displacement and sensor readings in voltage changes, making this stage the most suitable for usage. The results in Fig. 3C shows slight differences in the sensors placed at the same locations on the two soft finger network, but consistent results are recorded. We found that this is caused by the fabrication errors and assembly inaccuracies, which can be improved with optimized engineering processing and sensor calibration shown in Fig. 4A. After normalization and linear fitting, the sensor can be regarded as a linear element that relates to the midpoint displacement in Fig. 4A. The R^2 value is within 0.9544 and 0.9887, which is acceptable for linear fitting. Therefore, this interval of the curve can be regarded as a linear variation that can be used for sensor integration.

Tactile sensing information is extracted by mapping the displacement readings from the optical sensors with the force measurement from the 6D FT sensors, as shown in Fig. 4C. The measured displacement-force relationship shows consistent results after long-hours of usage and the reliable linear performance from previous experiments. We found the data was almost the same for any finger after the calibration and sorting experiments for two weeks. Therefore, by using the results in Figs. 3C and Fig. 4C, one can derive the force

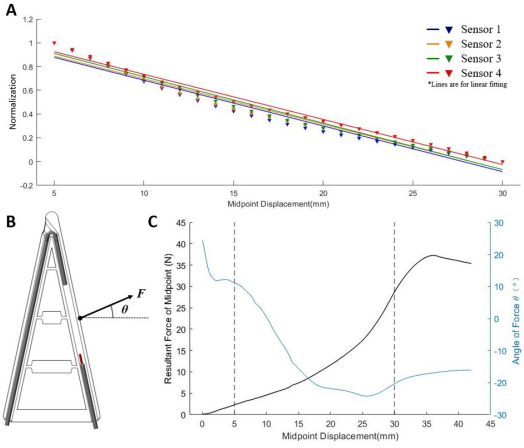

Fig. 4: Linear fitting in the interval of 5mm to 30mm (A). Magnitude and angle of the contact force at midpoint (B) of single-finger module change with displacement (C).

information of the soft finger structure during the interaction. Alternatively, one can also detect the hardness to measure the strain under a constant force. Basically, The softer the object is, the greater the strain will be.

IV. Object Sorting

As shown in Fig. 1, we propose a dual-finger design to replace the existing gripper's rigid finger. The OnRobot RG6 is adopted for modification with two sets of the dual-finger structure. The RG6 is selected for its relatively broader range of grasping and heavy payload design. One can easily modify the base mount design to install the proposed soft finger on almost any robot gripper with rigid fingers as a scalable solution.

For the object sorting task, both YCB objects [21] and some other routine objects are chosen for experiments. A microcomputer (Arduino NANO) is integrated with the fiber-cavity sensors on the gripper to send all sensor values to the upper computer by a serial port in real-time. The grasping force of RG6 needs to be set by users, but RG6 will measure and feedback the current width of the gripper. The additional sensing capability introduced by the fiber-cavity sensor enables further refined control of the grasping process by estimating the interaction force and shape the geometry of the objects in contact. The actual sectional diameter of the object under specific force theoretically equals to the estimated midpoint displacement plus the width of RG6 at the beginning contact point. Moreover, the actual strain of the object can be calculated by measuring the width of the object at both beginning contact state and final steady-state.

A. Calibration

Calibration of the sensor needs to transfers the raw measurement of the electronics data into intuitive information of real values. To do so, we use a series of plates with different standard widths to calibrate the gripper (Fig. 5A). Although the resolution of the sensor is less than 0.2mm, the inaccuracy is beyond this range. Therefore, we implement the calibration process by letting the gripper grasp the plates with standard width and record the sensor value. After obtaining a group of data, the linear fitting will be used to obtain a proportional relationship as the calibrated result of the sensor. So, any sensor readings will be transferred to the midpoint displacement via the calibrated expression.

B. Sorting Experiment

Some objects with different sizes and compliance were selected in the sorting experiment in Fig. 5B. One obvious challenge to distinguish objects with sectional diameters similar to each other. However, this is not common in the YCB object sets used in our experiment. We adopt a qualitative measurement of the object's hardness in a way similar to human grasping, where a scalar level of hardness is adopted.

It should be noted that more accurate measurement is always preferable, yet different grasping compliance may occur when approached from different angles. So the strains

Fig. 5: Fast calibration for gripper in a real application (A). A selection of sorting objects are selected from the YCB dataset and daily objects (B). Due to the parallel finger configuration used in our experiment, some objects (C) may slip through the gap between dual-fingers during grasping.

of samples under a positive force were manually determined by observing and simple measuring. The standard strains of samples are not accurate, but following the common sense of human, which can be used to judge the estimated strain. For object classification, our experiment requires the gripper to squeeze the object to determine these geometric features for sorting, which is similar to the human when visual data is not available or sufficiently enough. In this way, if the force applied to the object is constant, the strain of the object will be different due to the different compliant characteristics. The strain of each object is the ratio of deformation and original width before being exerted in a specific force. The ratio should be different to distinguish the objects (Fig. 6).

C. Result

The results are reported in Fig. 6, where we explore the basic discernibility of the gripper for width and compliance. The total amount of sample objects is 42. The green triangular marks, as shown in Fig. 6A are nine softest objects whose estimated diameters are much smaller than the actual diameters because their structures or materials cannot support the finger force. The orange diamond marks are the two balls whose diameters adapt the finger space but will cause the lateral bending and torsion of the finger. The lateral bending will result in the underestimate of the diameter in the sagittal plane. The black square mark is the result of a container of glass cleaner. The overestimate error happened because once a pair of fingers contact the bigger diameter of the bottle, it will prevent the other pair of fingers from contacting the smaller part. Thus, one result is typical, but the other is abnormal. Their strain cannot measure eight objects because the midpoint displacement did not reach a valid interval from 5mm to 30mm. The total amount of objects whose diameter and compliance can be correctly measured is 28 in 38, so the success rate of object classification is 73.7%.

Expect the soft objects, balls, and irregular objects, 94% of results from the rest 26 objects are in the range of $\pm$6mm with respect to absolutely accurate, as shown in Fig. 6A. The average error of the estimated diameter is 3.17mm. The result

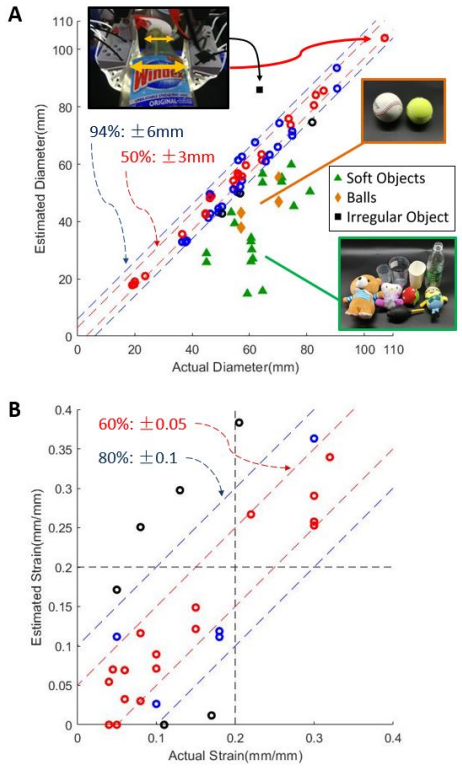

Fig. 6: Comparison of actual object properties with senor estimated properties. The estimated sectional diameter showed a nearly linear relationship with the actual diameter (A). 94% of rigid objects are within the error of ±6mm, expect the abnormal objects. The estimated strain, which represents the compliance of the object, has a relative consistency with the actual strain (B). The cross line is the soft-rigid boundary. The upper-right part is soft objects, and the lower-left part is rigid objects.

comes from the sectional diameter measured by two pairs of fiber-cavity sensors. There have four pairs of sensors, but we only use the two intermediate pairs of sensors to ensure the fingers entirely contact the objects, and the shape of the object passively drives the finger.

Twenty-eight objects have appropriate data to estimate strain from total graspable 38 objects. The result was shown in Fig. 6B. We cannot get an accurate conclusion as the actual strains are an intuitive perception of humans, but qualitative analysis is possible. The black dashed cross line is the boundary of rigid and soft according to the experiment. The objects in the upper-right section are deformable, such as plush toys. The objects in the lower-left section are rigid. The average error of the estimated strain is 0.062mm/mm. Some objects cannot induce enough deformation of the finger, which cannot calculate the strain via sensor data. So, for those objects, we consider them as unrecognizable samples. The estimated strain can be used to describe the hardness of an object because the grasping force is always the same. With the increase of strain, the objects become softer.

V. Discussion

A. Scalable Integration of Omni-adaptive Soft Finger

The scalability of the fiber-cavity sensory gripper is its most exceptional merit. First, the whole strategy is low-cost and straightforward the total cost of the four-fingers gripper with eight fiber-cavity sensors and one microcomputer (Fig. 1E) is less than 8 US dollars and the time of assembling all sensors into one 3D-printed finger is less than one minute. Thus, the modular sensory fingers could be as daily using or even more short-term use. Second, the structure could be used in many aspects, not only in the grasping area, and with the changing of the whole shape, sensor strategy can quickly adapt to the new shape without modification. For example, it can be used as a wheel to adapt the topography or an exoskeleton to adapt the wearer's body. Third, current fingers do not need to embed circuits, so working in a wet environment is its additional merit. Integrating these merits above, one of the most suitable working cases is in waste sorting. We do not need to consider the water in garbage and sterilization and disinfection method for the finger. Forth, the soft material and flexible structure could enable any rigid gripper a kind of omni-adaptability, and the scalable fiber-cavity sensor enables it a tactile sense. At last, the fiber-cavity sensor still has great potential because of high distinguishability and sensitivity after calibrating.

B. Enabling Design for Omni-adaptation

A major advantage of such a soft finger network is the ease of integration with existing gripper designs. By replacing the fingertips with this soft finger network, almost any rigid gripper is instantly enabled with passive adaptation with superior performance in all contact directions, such as the one shown in Fig. 1. Further discussion of this finger design is beyond the scope of this paper. In this paper, we aim at utilizing such geometric adaptation to integrate a sensing solution within the finger network structure.

C. Engineering Application for Object Sorting

Our current fiber-cavity sensory gripper could be improved further. First, the ambient light could impact the sensor values as the material is not lightproof. Although the calibrating operations could eliminate the influence, the change of light after calibration still impact the sensor. The receiving optical fiber is black coated, so the transparency of the white TPU causes the sensitivity to ambient light. Second, the inconsistency of the fiber-cavity sensor due to the fabricating process is a problem, though a temporary solution to the normalizing process could unify the curves. The 3D-printed TPU finger has defects and burrs on the inner tube wall that also affect the light transmission. Third, to pursue extremely low-cost, high sensitivity in the weak light environment and wide sensing range, we apply photoresistors as our underlying sensory elements. However, the inconsistency of the element, temperature-dependent, and non-linear properties are its drawbacks.

The drawbacks of the current fiber-cavity sensor are not insoluble. For the sensitivity of ambient light, a grey or black

colored TPU material, or just coat, a light-absorption layer could reduce transmissivity widely. For the inconsistency of the fiber-cavity sensor, we are trying to use casting to manufacture the finger whose surface is smooth and subtle. Besides, we will try to use some photoresistors with higher accuracy or find an appropriate photodiode.

The result of estimating diameter (Fig. 6A) is significant for further work because the precise regulation for the soft object shows the potential of fusion of visual and tactile sensing. An extra camera can fast measure the visual diameter, but the material is unknowable. With the fiber-cavity sensor, we can estimate hardness as the softer objects will have more differences between the visual size and physical size.

As for the result of estimating strain (Fig. 6A), the quantitative conclusion is inaccurate. There are three possible reasons. First, the standard strains of specific objects are measured by human perception. We ensured the rank of each object's strain was correct but were unable to guarantee that the absolute value was correct. So, the distribution of points is scattered, but the tendency of points basically concentrates in the correct area. The conclusion of 'soft' or 'rigid' for a particular object is correct according to the value of sensors and the soft-rigid boundary. Second, we think the sensor is accurate in the range of 5-30mm, but some objects cannot reach 5mm of midpoint displacement, because their structural shape limits the bending of fingers, whose contact points are at the tips of fingers. Third, the compliance of 3D-printed finger are inconsistent, and the sectional diameter of the object is variable, both of which result in the heterogeneous force while grasping. However, for human perception, the hardness of an object is a scale rather than a numerical value, so we consider the result is useful as the tendency is correct.

VI. Final Remarks

In this paper, we demonstrated a scalable bending sensor method for a novel design of omni-adaptive soft robotic fingers. Our work combined the omni-adaptive finger and fiber-cavity sensor to enable more functions based on its structure. Furthermore, we implemented experiments to find the relationship between midpoint displacement and sensor value. We demonstrated their nearly linear relationship in the interval of 5mm to 30mm, which could be used to calibrate the gripper and estimate the actual width and compliance of objects in sorting tasks. The final result of sorting showed the estimated widths of 94% objects are within $\pm$6mm error, and the estimate strains of 80% objects are within $\pm$0.1mm/mm. The object identification rate from a total of 38 objects from the YCB dataset and some other objects covering basic routine things is 73.7%.

Future work on this sensory gripper will focus on the improvement of the fiber-cavity sensor and application in multi-tasking. We will continue to develop the advantages of low-cost and modular design, meanwhile, to improve the performance of the fiber-cavity sensor. Our next application scenarios are for waste sorting, which needs the properties of omni-adaptive, waterproof, low-cost, and easy-replaced. We want to combine the computer vision and neural network to complete a more perceptive model of the finger and build a system to learn how to grasp new objects through training.

References

[1] C. Laschi, B. Mazzolai, and M. Cianchetti, "Soft robotics: Technologies and systems pushing the boundaries of robot abilities," *Science Robotics*, vol. 1, no. 1, 2016. [Online]. Available: https://robotics.sciencemag.org/content/1/1/eaah3690

[2] H. Wang, M. Totaro, and L. Beccai, "Toward perceptive soft robots: Progress and challenges," *Advanced Science*, vol. 5, no. 9, p. 1800541, 2018.

[3] T. G. Thuruthel, B. Shih, C. Laschi, and M. T. Tolley, "Soft robot perception using embedded soft sensors and recurrent neural networks," *Science Robotics*, vol. 4, no. 26, p. eaav1488, 2019.

[4] Z. Wang and S. Hirai, "Soft gripper dynamics using a line-segment model with an optimization-based parameter identification method," *IEEE Robotics and Automation Letters*, vol. 2, no. 2, pp. 624–631, 2017.

[5] N. Tan, X. Gu, and H. Ren, "Simultaneous robot-world, sensor-tip, and kinematics calibration of an underactuated robotic hand with soft fingers," *IEEE Access*, vol. 6, pp. 22 705–22 715, 2017.

[6] D. Rus and M. T. Tolley, "Design, fabrication and control of soft robots," *Nature*, vol. 521, no. 7553, p. 467, 2015.

[7] P. Boonvisut and M. C. Çavuşoğlu, "Estimation of soft tissue mechanical parameters from robotic manipulation data," *IEEE/ASME Transactions on Mechatronics*, vol. 18, no. 5, pp. 1602–1611, 2012.

[8] P. A. Xu, A. Mishra, H. Bai, C. Aubin, L. Zullo, and R. Shepherd, "Optical lace for synthetic afferent neural networks," *Science Robotics*, vol. 4, no. 34, p. eaaw6304, 2019.

[9] J. G. da Silva, A. A. de Carvalho, and D. D. da Silva, "A strain gauge tactile sensor for finger-mounted applications," *IEEE Transactions on Instrumentation and measurement*, vol. 51, no. 1, pp. 18–22, 2002.

[10] L. Chin, M. C. Yuen, J. Lipton, L. H. Trueba, R. Kramer-Bottiglio, and D. Rus, "A simple electric soft robotic gripper with high-deformation haptic feedback," in *International Conference on Robotics and Automation*, 2019.

[11] H. Zhao, K. O'Brien, S. Li, and R. F. Shepherd, "Optoelectronically innervated soft prosthetic hand via stretchable optical waveguides," *Science Robotics*, vol. 1, no. 1, p. eaai7529, 2016.

[12] M. Park, B.-G. Bok, J.-H. Ahn, and M.-S. Kim, "Recent advances in tactile sensing technology," *Micromachines*, vol. 9, no. 7, p. 321, 2018.

[13] S. Sundaram, P. Kellnhofer, Y. Li, J.-Y. Zhu, A. Torralba, and W. Matusik, "Learning the signatures of the human grasp using a scalable tactile glove," *Nature*, vol. 569, no. 7758, p. 698, 2019.

[14] I. Van Meerbeek, C. De Sa, and R. Shepherd, "Soft optoelectronic sensory foams with proprioception," *Science Robotics*, vol. 3, no. 24, p. eaau2489, 2018.

[15] S. Stassi, V. Cauda, G. Canavese, and C. F. Pirri, "Flexible tactile sensing based on piezoresistive composites: A review," *Sensors*, vol. 14, no. 3, pp. 5296–5332, 2014.

[16] J. I. Lipton, R. MacCurdy, Z. Manchester, L. Chin, D. Cellucci, and D. Rus, "Handedness in shearing auxetics creates rigid and compliant structures," *Science*, vol. 360, no. 6389, pp. 632–635, 2018.

[17] D. Sartiano and S. Sales, "Low cost plastic optical fiber pressure sensor embedded in mattress for vital signal monitoring," *Sensors*, vol. 17, no. 12, p. 2900, 2017.

[18] J. Shintake, V. Cacucciolo, D. Floreano, and H. Shea, "Soft robotic grippers," *Advanced Materials*, vol. 30, no. 29, p. 1707035, 2018.

[19] R. L. Truby, R. K. Katzschmann, J. A. Lewis, and D. Rus, "Soft robotic fingers with embedded ionogel sensors and discrete actuation modes for somatosensitive manipulation," in *2019 2nd IEEE International Conference on Soft Robotics (RoboSoft)*. IEEE, 2019, pp. 322–329.

[20] L. Chin, J. Lipton, M. C. Yuen, R. Kramer-Bottiglio, and D. Rus, "Automated recycling separation enabled by soft robotic material classification," in *2019 2nd IEEE International Conference on Soft Robotics (RoboSoft)*. IEEE, 2019, pp. 102–107.

[21] B. Calli, A. Singh, A. Walsman, S. Srinivasa, P. Abbeel, and A. M. Dollar, "The ycb object and model set: Towards common benchmarks for manipulation research," in *2015 international conference on advanced robotics (ICAR)*. IEEE, 2015, pp. 510–517.